DOI: 10.1002/chem.200903282

Stabilization of HHeF by Complexation: Is it a Really Viable Strategy?

Maria Giordani,[a] Paola Antoniotti,[b] and Felice Grandinetti*[a]

Abstract: Ab initio calculations at the MP2 and CCSD(T) levels of theory have disclosed the conceivable existence of fluorine-coordinated complexes of HHeF with alkali-metal ions and molecules M^+ ($M^+ = Li^+$–Cs^+), M^+–OH_2, M^+–NH_3 ($M^+ = Li^+$, Na^+), and MX (M = Li, Na; X = F, Cl, Br). All these ligands L induce a shortening of the H–He distance and a lengthening of the He–F distance accompanied by consistent blue- and redshifts, respectively, of the H–He and He–F stretching modes. These structural effects are qualitatively similar to those predicted for other investigated complexes of the noble gas hydrides HNgY, but are quantitatively more pronounced. For example, the blueshifts of the H–He stretching mode are exceptionally large, ranging between around 750 and 1000 cm^{-1}. The interactions of HHeF with the ligands investigated herein also enhance the $(HHe)^+$ F^- dipole character and produce large complexation energies of around 20–60 kcal mol^{-1}. Most of the HHeF–L complexes are indeed so stable that the three-body dissociation of HHeF into H + He + F, exothermic by around 25–30 kcal mol^{-1}, becomes endothermic. This effect is, however, accompanied by a strong decrease in the H–He–F bending barrier. The complexation energies, ΔE, and the bending barriers, E^*, are, in particular, related by the inverse relationship $E^*(\text{kcal mol}^{-1}) = 6.9\exp[-0.041\Delta E(\text{kcal mol}^{-1})]$. Therefore the HHeF–L complexes, which are definitely stable with respect to H + He + F + L ($\Delta E \approx 25$–30 kcal mol^{-1}), are predicted to have bending barriers of only 0.5–2 kcal mol^{-1}. Overall, our calculations cast doubt on the conceivable stabilization of HHeF by complexation.

Keywords: ab initio calculations · fluorine · helium · noble gases · structure–property relationships

Introduction

The chemistry of the noble gases is currently enjoying an upsurge in interest,[1] stimulated by the recent discovery of unprecedented compounds and bonding motifs.[2–8] The noble gas hydrides HNgY (Ng = noble gas atom; Y = electronegative fragment) constitute, in particular, a important part of modern noble gas chemistry.[9,10] These molecules are prepared by photodissociation of HY in a cold Ng matrix and subsequent mobilization of the hydrogen atoms. Species already observed include HArF, the only argon compound,[11,12] nearly 20 HKrY and HXeY species,[10] and the dinuclear compounds HXeCCXeH[13] and HXeOXeH.[14,15]

[a] Dr. M. Giordani, Prof. F. Grandinetti
Dipartimento di Scienze Ambientali, Università della Tuscia
L.go dell' Università, s.n.c., 01100 Viterbo (Italy)
Fax: (+39) 0761-357179
E-mail: fgrandi@unitus.it

[b] Dr. P. Antoniotti
Dipartimento di Chimica Generale e Chimica Organica
Università degli Studi di Torino
C.so M. d'Azeglio, 48, 10125 Torino (Italy)

In 2000, Wong predicted the conceivable existence of HHeF.[16] This species still remains the only candidate for a covalent compound of the lightest noble gases, and the conditions for its stabilization have therefore been investigated in considerable detail.[17–27] All the calculations predict that HHeF has a very compact structure with short bond lengths and high harmonic frequencies. The dissociations shown in reactions (1) and (2) are, however, largely exothermic and HHeF can therefore exist only as a metastable species. At the multi-reference configuration interaction level of theory with triple-zeta basis sets and without the inclusion of zero-point energies (ZPE), the energy changes of reactions (1) and (2) are estimated to be −0.721 and −6.831 eV, respectively.[19] The lifetime of HHeF, first predicted as 120 ps (14 ns for DHeF),[18] was subsequently revised to only 157 fs.[19] This small value essentially reflects the fast occurrence of reaction (1), a collinear dissociation process with a barrier of 0.224 eV (with no ZPE).[19] Reaction (2) occurs instead by a bending motion and has a higher activation barrier (with no ZPE) of 0.448 eV.[19] The intrinsic instability of HHeF stimulated interest in its conceivable stabilization by environmental effects. It was thus predicted[20] that at pressures above 15 GPa a solid helium matrix could completely

block reactions (1) and (2) and make HHeF indefinitely stable. The required experiments are however extremely challenging[9] and it became of interest to investigate whether complexation effects could still stabilize HHeF in cold matrices.[24–27] In general, a first requisite for a ligand L to stabilize HHeF is that the complexation energy of (HHeF)L is larger than the energy change of reaction (1), namely, around 25 kcal mol^{-1} (including the ZPE). All the HNgY species observed to date are in fact theoretically more stable than H+Ng+Y.[10,28] A ligand L can also affect the stability of HHeF with respect to reaction (2). The only evidence in this regard is that a single xenon atom slightly decreases the bending barrier.[24] In addition, the bending barriers of HArF complexed to HF[29,30] and of HXeOH clustered with water molecules[31] are lower than the bending barriers of HArF and HXeOH.

$$HHeF \rightarrow H + He + F \quad (1)$$

$$HHeF \rightarrow He + HF \quad (2)$$

The complexes of HHeF with noble gas atoms,[24,27,32] N_2,[25,32] and CO[26,32] are hydrogen-bonded structures with complexation energies of only 1–3 kcal mol^{-1}. It has been suggested that large xenon clusters or matrices could suppress the dissociation of HHeF along the stretching mode,[24] but this stabilization by bulk effects has not been directly supported by calculations. In their equilibrium geometries, the noble gas hydrides HNgY feature a covalent H–Ng bond and a strong ionic interaction, best described by the resonance form $(H–Ng)^+Y^-$.[9,10] The charge separation of HHeF is, in particular, predicted to be as large as around $+0.65e/-0.65e$,[21] and one expects that electrophilic ligands L bind to the fluorine atom of HHeF to form HHeF–L complexes. Such fluorine-coordinated structures are, however, still unreported. In this computational study, we found that alkali-metal ions and molecules bind to the fluorine atom of HHeF with complexation energies that range between around 20 and 60 kcal mol^{-1}. These values are, in general, large enough to stabilize HHeF with respect to H+He+F. However, this thermochemical stabilization is invariably accompanied by an appreciable lowering of the H–He–F bending barrier, which is predicted to be between only 0.5 and 3 kcal mol^{-1}. We discuss herein the properties of our investigated HHeF–L complexes, the relationships between their complexation energies and bending barriers, and the implications of these results for the conceivable stabilization of HHeF by complexation.

Results and Discussion

Structures and harmonic frequencies: The naked and solvated alkali-metal ions M^+ ($M^+ = Li^+–Cs^+$), $M^+–OH_2$, and $M^+–NH_3$ ($M^+ = Li^+$, Na^+), and the alkali-metal halides MX (M = Li, Na; X = F, Cl, Br) bind to HHeF to form the fluorine-coordinated complexes shown in Figure 1.[33]

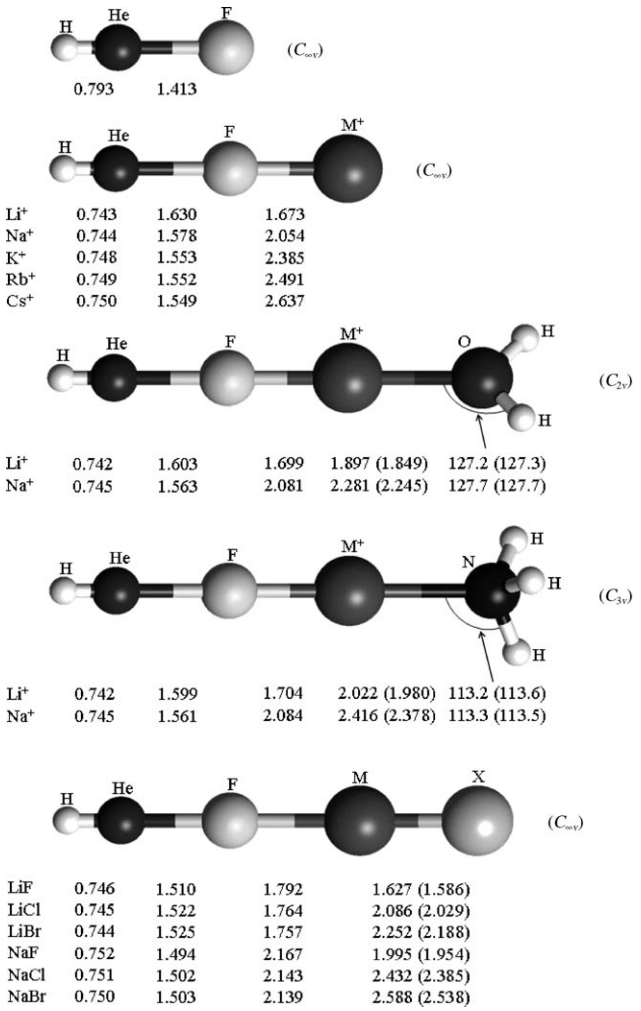

Figure 1. MP2(full)/6-311++G(2d,2p)/SDD optimized geometries (bond lengths in Å and angles in °) of the HHeF–L complexes. The parameters of the free ligands L are given in parentheses.

All these species were characterized as true minima on the MP2(full)/6-311++G(2d,2p)/SDD potential energy surface and their CCSD T1 diagnostics[34] were invariably within the threshold of 0.02. This suggests that they should be, in general, well described by single-reference methods. We reoptimized the geometries of the exemplary HHeF–M^+ complexes ($M^+ = Li^+–Cs^+$) at the MP2(full)/def2-TZVPP level of theory and also recalculated the bond lengths of HHeF–Li^+ and HHeF–LiF at the CCSD(T,full)/aug-cc-pVTZ level of theory. In all cases, we noticed only minor differences with the MP2(full)/6-311++G(2d,2p) absolute values and geometric trends.

The fluorine complexation of HHeF is invariably accompanied by a shortening of the H–He distance and a lengthening of the He–F distance. The H–He distance is shortened by around 0.04–0.05 Å and is only little affected by the nature of the ligand L. It is, however, still possible to recognize, for example, the periodic increase of the effect on pass-

ing from HHeF–Li^+ to HHeF–Cs^+. The lengthening of the He–F distance is instead more appreciable and, in general, more pronounced for the cationic rather than the neutral ligands. The largest elongations produced by M^+ ($M^+ = Li^+$–Cs^+) range from 0.217 (Li^+) to 0.136 Å (Cs^+) and decrease in the periodic order $Li^+ > Na^+ > K^+ \sim Rb^+ > Cs^+$. The solvated ions M^+–OH_2 and M^+–NH_3 ($M^+ = Li^+$, Na^+) still lead to an increase in the He–F bond length of HHeF, but less than with the naked cations. We also note that the effect is inversely related to the nucleophilicity of the solvating molecule, namely, M^+–$NH_3 < M^+$–OH_2. The optimized geometries of HHeF–Li^+–Nu and HHeF–Na^+–Nu (Nu = H_2O, NH_3) also indicate that the solvation of HHeF–M^+ elongates the F–M bond and that this effect is larger for the more nucleophilic ligand NH_3. The neutral LiX and NaX (X = F, Cl, Br) lengthens the He–F distance of HHeF by around 0.1 Å and, for any X, the predicted elongations follow the periodic trend LiX > NaX (X = F, Cl, Br). In addition, for both LiX and NaX, the effect slightly decreases in the order Br > Cl > F. We also note that the coordination of any M^+–OH_2, M^+–NH_3, and MX (M = Li, Na; X = F, Cl, Br) to the fluorine atom in HHeF lengthens the M–O, M–N, and M–X distances of the free ligands by around 0.04–0.05 Å.

The structural changes in HHeF induced by fluorine complexation are invariably accompanied by consistent shifts of the harmonic frequencies. The relevant data are reported in Table 1.

We note, in particular, the exceptionally large blueshift (increase in the harmonic frequency and decrease in the IR intensity) of the H–He stretching mode, computed to be between around 750 and 1000 cm^{-1}, and the still large redshift (decrease in the harmonic frequency and increase in the IR intensity) of the He–F stretching mode, computed to be between around 130 and 370 cm^{-1}. The H–He–F bending mode is also redshifted by around 140–330 cm^{-1}. The largest and lowest effects are invariably predicted, respectively, for the lithium cationic complexes HHeF–Li^+ and HHeF–Li^+–Nu (Nu = H_2O, NH_3), and for the sodium neutral complexes HHeF–NaX (X = F, Cl, Br). Interestingly, the blueshift of the H–He stretching mode and the redshift of the He–F stretching mode are nearly linearly related to the shortening of the H–He distance and to the lengthening of the He–F distance, respectively. These correlations are shown in Figures 2 and 3.

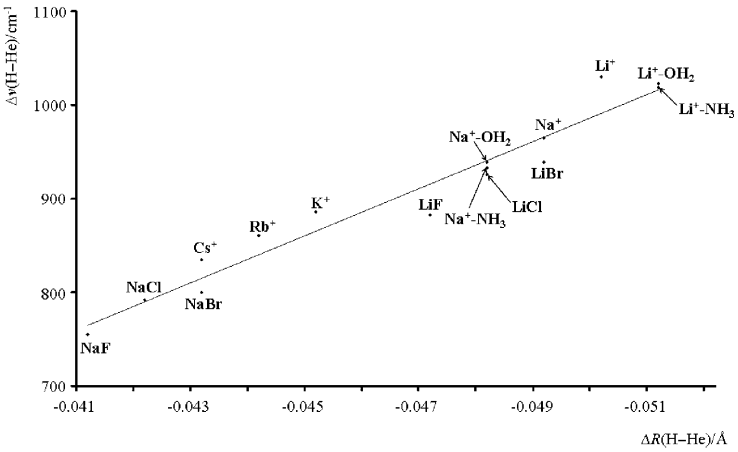

Figure 2. MP2(full)/6-311++G(2d,2p)/SDD blueshift of the H–He stretching mode versus shortening of the H–He bond length by fluorine complexation of HHeF with the specified ligands.

Complexation energies and stabilities: To evaluate the stabilities of the HHeF–L complexes, we calculated the energy changes, ΔE, at 0 K of the dissociations shown in reactions (3a), (3b), and (3c).

$$\text{HHeF–L} \rightarrow \text{HHeF} + \text{L} \quad (3a)$$

$$\text{HHeF–L} \rightarrow \text{H} + \text{He} + \text{F} + \text{L} \quad (3b)$$

$$\text{HHeF–L} \rightarrow \text{He} + \text{HF} + \text{L} \quad (3c)$$

For the cationic HHeF–M^+ ($M^+ = Li^+$–Cs^+), we also explored its conceivable rupture into HHe^+ and MF. The results obtained by single-point calculations at the CCSD(T,full)/6-311++G(3df,3pd)/SDD level of theory are reported in Table 2.

The complexation energies, ΔE(3a), range between 19.8 (L = NaF) and 61.6 kcal mol^{-1} (L = Li^+) and follow the peri-

Table 1. MP2(full)/6-311++G(2d,2p)/SDD harmonic frequencies and frequency shifts [cm^{-1}] of the HHeF–L complexes (see Figure 1). IR intensities [km mol^{-1}] are given in parentheses.

L	ν(H–He)	$\Delta\nu$(H–He)	ν(He–F)	$\Delta\nu$(He–F)	δ(H–He–F)[a]	$\Delta\delta$(H–He–F)
None	2702 (2952)		1006 (509)		829 (38)	
Li^+	3732 (99)	+1030 (−2853)	640 (84)	−366 (−425)	503 (148)	−326 (110)
Li^+–OH_2	3725 (35)	+1023 (−2917)	700 (154)	−306 (−355)	551 (140)[b]	−278 (102)
					553 (141)[c]	−276 (103)
Li^+–NH_3	3721 (27)	+1019 (−2925)	699 (119)	−307 (−390)	555 (145)	−274 (107)
Na^+	3667 (0)	+965 (−2952)	751 (544)	−255 (35)	598 (123)	−231 (85)
Na^+–OH_2	3641 (11)	+939 (−2941)	770 (572)	−236 (63)	606 (120)[b]	−223 (82)
					607 (118)[c]	−222 (80)
Na^+–NH_3	3635 (15)	+933 (−2937)	773 (585)	−233 (76)	615 (117)	−214 (79)
K^+	3588 (59)	+886 (−2893)	778 (609)	−228 (100)	642 (110)	−187 (72)
Rb^+	3563 (89)	+861 (−2863)	776 (650)	−230 (141)	639 (106)	−190 (68)
Cs^+	3537 (147)	+835 (−2805)	776 (703)	−230 (194)	643 (103)	−186 (65)
LiF	3585 (183)	+883 (−2769)	858 (636)	−148 (127)	672 (99)	−157 (61)
LiCl	3628 (117)	+926 (−2835)	841 (708)	−165 (199)	648 (101)	−181 (63)
LiBr	3641 (101)	+939 (−2851)	836 (727)	−170 (218)	642 (102)	−187 (64)
NaF	3457 (436)	+755 (−2516)	875 (621)	−131 (112)	682 (88)	−147 (50)
NaCl	3494 (376)	+792 (−2576)	864 (656)	−142 (147)	686 (90)	−143 (52)
NaBr	3502 (368)	+800 (−2584)	861 (673)	−145 (164)	680 (90)	−149 (52)

[a] Doubly-degenerate bending motion. [b] B_1 symmetry. [c] B_2 symmetry.

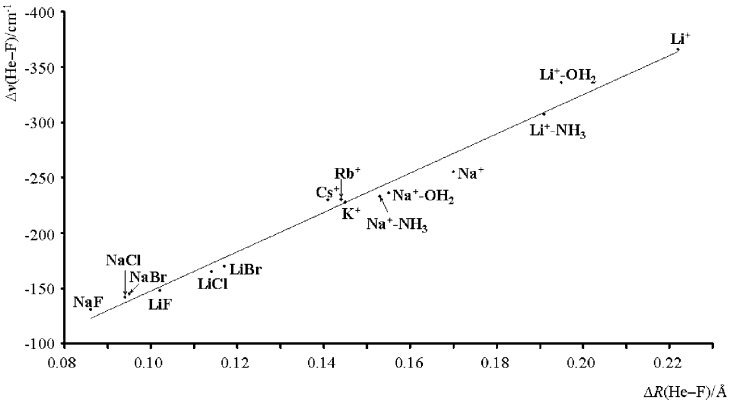

Figure 3. MP2(full)/6-311++G(2d,2p)/SDD redshift of the He–F stretching mode versus lengthening of the He–F bond by complexation of HHeF with the specified ligands.

Table 2. CCSD(T,full)/6-311++G(3df,3pd)/SDD//MP2(full)/6-311++G(2d,2p)/SDD dissociation energies at 0 K for the HHeF–L complexes (reference species). The values in parentheses do not include the BSSE.

L	Dissociation energy [kcal mol^{-1}]				E*[a]
	HHeF+L	HHe$^+$+MF	H+He+F+L	He+HF+L	[kcal mol^{-1}]
None			−27.9 (−26.2)	−161.3	6.9 (1304i)
Li^+	61.6 (63.6)	58.4 (59.3)	34.3 (37.4)	−97.7	0.5 (678i)
Li^+–OH_2	52.8 (55.4)		25.5 (29.2)	−105.9	0.8 (729i)
Li^+–NH_3	51.6 (54.1)		24.3 (27.9)	−107.2	0.8 (738i)
Na^+	44.7 (46.6)	61.2 (62.5)	17.3 (20.4)	−114.7	1.3 (808i)
Na^+–OH_2	39.7 (41.6)		12.2 (15.4)	−119.7	1.6 (839i)
Na^+–NH_3	38.9 (40.8)		11.5 (14.6)	−120.5	1.6 (846i)
K^+	35.0 (35.9)	67.1 (68.3)	7.4 (9.7)	−125.4	1.9 (887i)
Rb^+	32.8 (33.8)	67.8 (68.5)	5.3 (7.6)	−127.5	2.2 (896i)
Cs^+	30.1 (31.1)	66.5 (67.7)	2.5 (4.9)	−130.2	2.3 (909i)
LiF	24.7 (27.3)		−2.8 (1.1)	−134.0	2.0 (923i)
LiCl	28.5 (31.1)		1.0 (4.9)	−130.2	1.8 (886i)
LiBr	29.3 (31.9)		1.8 (5.7)	−129.4	1.7 (875i)
NaF	19.8 (21.6)		−7.8 (−4.6)	−139.7	3.0 (993i)
NaCl	22.0 (23.9)		−5.6 (−2.3)	−137.4	2.6 (972i)
NaBr	22.4 (24.3)		−5.2 (−1.9)	−137.0	2.6 (967i)

[a] Energy barrier at 0 K for the decomposition HHeF–L→He+HF+L. The single imaginary frequency of the corresponding TS is given in parentheses.

odic trends $Li^+ > Na^+ > K^+ > Rb^+ > Cs^+$ and LiX > NaX (X = F, Cl, Br). In addition, for both LiX and NaX, they regularly decrease in the order Br > Cl > F. Interestingly, these variations strictly parallel the trends in the geometric changes and frequency shifts of HHeF induced by complexation. The regular decrease in the complexation energies of HHeF with M^+ ($M^+ = Li^+$–Cs^+) is consistent with the periodic trends of the alkali metal ion affinities of numerous nucleophiles.[35–38] It is also established that solvated alkali metal ions are, in general, weaker Lewis acids than the naked cations.[37,39,40] For example, passing from Li^+ and Na^+ to Li^+–OH_2 and Na^+–OH_2, the complexation energies with water decrease by around 8 and 4 kcal mol^{-1}, respectively.[39] Similarly, passing from Li^+ and Na^+ to Li^+–NH_3 and Na^+–NH_3, the complexation energies with ammonia decrease by around 5 and 3 kcal mol^{-1}, respectively.[40] Interestingly, we note from Table 2 that on passing from Li^+ and Na^+ to Li^+–Nu and Na^+–Nu (Nu = H_2O, NH_3) the complexation energies with HHeF are reduced by around 5–10 kcal mol^{-1}. On the other hand, the absolute complexation energies of HHeF are apparently larger than expected from qualitative arguments. For example, at the CCSD(T) level of theory with a triple-zeta basis set,[41] the Li^+ affinity of HF is 22.2 kcal mol^{-1}, significantly lower than the Li^+ affinities of H_2O (33.1 kcal mol^{-1}) and NH_3 (38.0 kcal mol^{-1}). We obtained in this work similar theoretical values of 24.3, 31.4, and 36.2 kcal mol^{-1}, respectively, which compare favorably with the experimental Li^+ affinities of H_2O (31.8 kcal mol^{-1}) and NH_3 (38.0 kcal mol^{-1}) at 0 K.[35] Our calculated Na^+ affinities of H_2O (21.9 kcal mol^{-1}) and NH_3 (25.0 kcal mol^{-1}) are also in very good agreement with the experimental values at 0 K of 22.6 and 24.4 kcal mol^{-1}, respectively.[36] We therefore regard the complexation energies listed in Table 2, in general, to be reasonably accurate and conclude that the alkali-metal-ion affinities of HHeF are remarkably large and are nearly twice the alkali-metal-ion affinities of H_2O. As discussed below, the interaction between the alkali-metal ligands and HHeF is of ion–dipole or dipole–dipole character. Taking into account the large dipole character of HHeF, even enhanced by complexation, it is not actually surprising that the complexation energies of the HHeF–L complexes are indeed particularly large.

For any cationic ligand and for the neutral ligands LiBr and LiCl, the values of ΔE(3a) are indeed so large that the dissociation reaction (3b) is endothermic. In contrast, for the neutral ligands LiF and NaX (X = F, Cl, Br), reaction (3b) is exothermic by 5–8 kcal mol^{-1}. All cationic HHeF–M^+ ($M^+ = Li^+$–Cs^+) species are also far more stable than HHe^+ and MF. On the other hand, all the HHeF–L complexes are largely unstable with respect to the loss of HF. The values of ΔE(3c) in fact range between −97.7 (L = Li^+) and −139.7 kcal mol^{-1} (L = NaF). However, similarly to HHeF, these dissociations are protected by the bent transition-state structures (TS) shown in Figure 4.

Similarly to the HHeF–L energy minima, the CCSD T1 diagnostics of these species are invariably within the threshold of 0.02. Passing from any minimum to the corresponding TS, the He–F bond length increases, the F–M bond length slightly decreases, and the H–He bond length remains essentially unchanged or only slightly decreases. The most important structural change required to overcome the activation barrier is, however, the closing of the H–He–F bond angle, which is invariably reduced by nearly 60°. The He–F–M bond angle remains instead essentially unchanged at around 180°. The activation barriers of reaction (3c), E*(3c), are significantly lower than that of HHeF (Table 2). They range in fact between 0.5 (L = Li^+) and 3.0 kcal mol^{-1} (L = NaF), whereas the bending barrier of HHeF is predicted to be 6.9 kcal mol^{-1}. We noticed in particular that these activation barriers and the complexation energies of the HHeF–L complexes, ΔE(3a), are related by Equation (6) ($r^2 = 0.95$)

$$E^*(3c) = 6.9\exp[-0.041\Delta E(3a)] \quad (4)$$

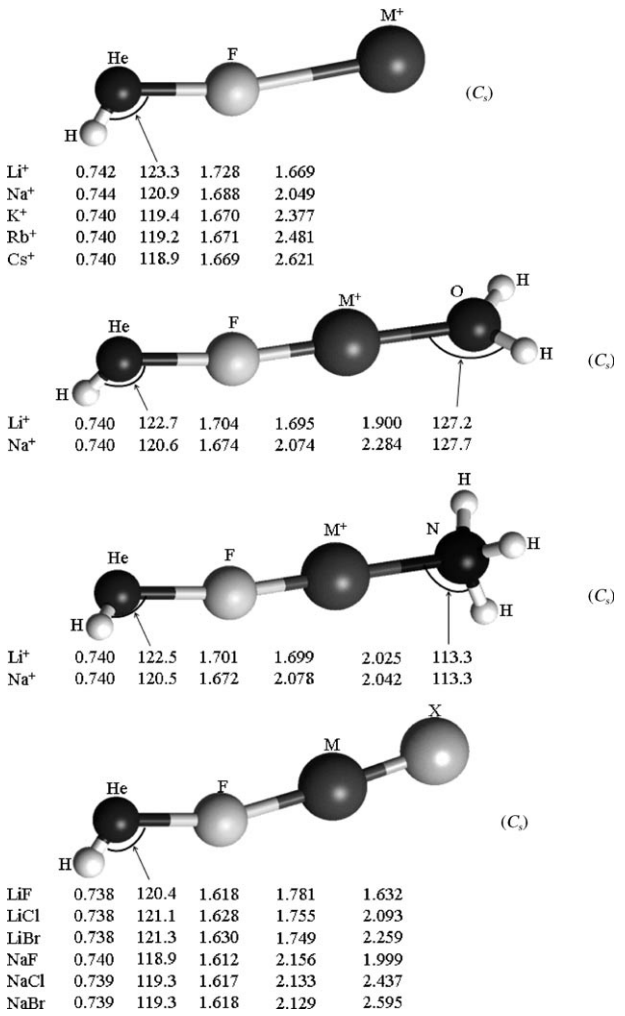

Figure 4. MP2(full)/6-311++G(2d,2p)/SDD optimized geometries (bond lengths in Å and angles in °) of the TS for the decomposition HHeF–L→He+HF+L.

The single points and the fitting curve are shown in Figure 5. The most relevant observation is that the HHeF–L complexes that reside in the "stability island" of HHeF with respect to H+He+F feature low bending barriers of only 0.5–2 kcal mol^{-1}. These species are therefore predicted to be hardly observable even in cold matrices. This finding has implications for the proposed stabilization of HHeF by complexation. In particular, if one assumes that Equation (4) is valid for any fluorine-coordinated complex of HHeF, our calculations, in general, cast doubt on the conceivable stabilization of HHeF by complexation. They show in fact that it is possible to find ligands that inhibit the three-body dissociation of HHeF, but that the ensuing HHeF–L complexes are intrinsically unstable with respect to the decomposition in reaction (3c). It is also known that hydrogen-coordinated complexes such as Ng–HHeF, N_2–HHeF, and CO–HHeF are too weakly bound to stabilize HHeF with respect to H+He+F.[24–27] It will certainly be of interest to search for novel fluorine-coordinated complexes of HHeF to definitely

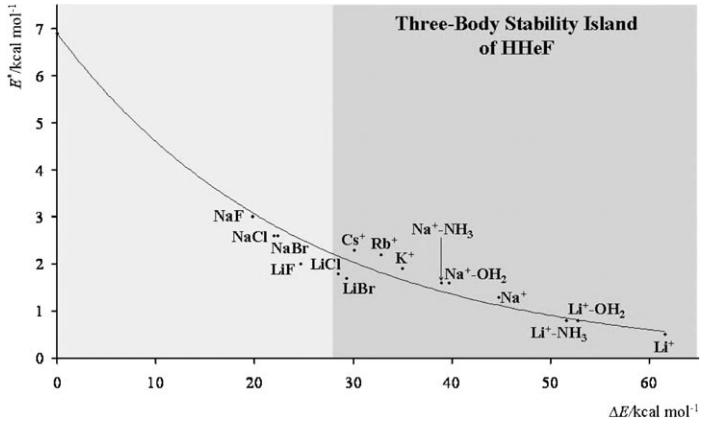

Figure 5. CCSD(T,full)/6-311++G(3df,3pd)/SDD//MP2(full)/6-311++G(2d,2p)/SDD activation barrier, E^*, for the decomposition HHeF–L→He+HF+L versus the complexation energy, ΔE, of HHeF with the specified ligands. In the dark zone, the dissociation HHeF–L→H+He+F+L is endothermic.

support or confute the general validity of Equation (4). The IRC calculations performed to characterize the TSs shown in Figure 4 revealed that, for the HHeF–M$^+$ complexes (M$^+$ = Li$^+$–Cs$^+$), reaction (3c) proceeds through an intermediate complex M$^+$–FH, which in turn dissociates with no barrier into M$^+$ and HF. Figure 6 shows the exemplary energy diagram for the decomposition of HHeF–Li$^+$.

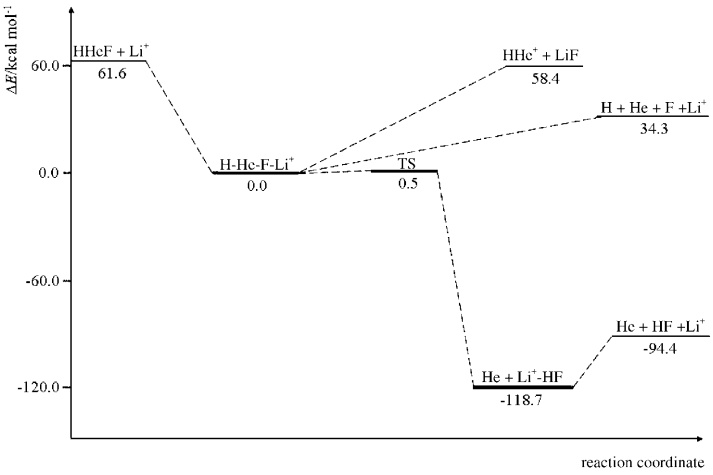

Figure 6. CCSD(T,full)/6-311++G(3df,3pd)//MP2(full)/6-311++G-(2d,2p) energy diagram for the decomposition HHeF–Li$^+$→He+HF+Li$^+$.

Charge distributions and bonding analysis: The charge distributions of the HHeF–L complexes and the results of the atoms-in-molecules (AIM) analysis are reported in Tables 3 and 4.

The fluorine complexation of HHeF invariably enhances the ion-pair character (HHe)$^+$F$^-$. The charge separation of HHeF, estimated to be $+0.69e/-0.69e$, increases up to

Table 3. MP2(full)/6-311++G(2d,2p)/SDD NBO atomic charges (e) of the HHeF–L complexes. The values in the free ligands are given in parentheses.

L	q(HHe)	q(He)	q(F)	q(M)[a]	q(X)[b]	q(H)
None	0.688	0.341	−0.688			
Li^+	0.931	0.321	−0.917	0.986 (+1)		
Li^+–OH_2	0.917	0.325	−0.899	0.966 (0.990)	−1.000 (−1.031)	0.508 (0.521)
Li^+–NH_3	0.915	0.326	−0.894	0.949 (0.978)	−1.131 (−1.172)	0.387 (0.398)
Na^+	0.899	0.329	−0.893	0.994 (+1)		
Na^+–OH_2	0.888	0.331	−0.880	0.985 (0.996)	−0.989 (−1.007)	0.498 (0.505)
Na^+–NH_3	0.888	0.331	−0.877	0.972 (0.984)	−1.117 (−1.139)	0.378 (0.385)
K^+	0.878	0.332	−0.872	0.994 (+1)		
Rb^+	0.875	0.332	−0.866	0.991 (+1)		
Cs^+	0.870	0.332	−0.861	0.991 (+1)		
LiF	0.857	0.342	−0.842	0.946 (0.957)	−0.961 (−0.957)	
LiCl	0.868	0.340	−0.846	0.907 (0.927)	−0.929 (−0.927)	
LiBr	0.872	0.340	−0.848	0.895 (0.915)	−0.919 (−0.915)	
NaF	0.832	0.342	−0.825	0.973 (0.978)	−0.980 (−0.978)	
NaCl	0.840	0.341	−0.831	0.944 (0.946)	−0.953 (−0.946)	
NaBr	0.843	0.341	−0.832	0.938 (0.936)	−0.947 (−0.936)	

[a] M = alkali metal. [b] X = O, N, F, Cl, Br.

Table 4. MP2(full)/6-311++G(2d,2p)/SDD AIM analysis of the HHeF–L complexes. The charge density, ρ [e Å^{-3}], and the Laplacian of the charge density, $\nabla^2\rho$ [e Å^{-5}] calculated at the bond critical point on the specified bond.

L	ρ(H–He)	$\nabla^2\rho$(H–He)	ρ(He–F)	$\nabla^2\rho$(He–F)	ρ(F–M)[a]	$\nabla^2\rho$(F–M)[a]	ρ(M–X)[a,b]	$\nabla^2\rho$(M–X)[a,b]
None	1.816	−47.547	0.926	14.338				
Li^+	1.817	−73.333	0.456	8.871	0.353	11.604		
Li^+–OH_2	1.846	−71.453	0.496	9.558	0.327	10.481	0.208	5.535
Li^+–NH_3	1.849	−71.164	0.501	9.647	0.324	10.266	0.204	4.290
Na^+	1.865	−68.297	0.539	10.165	0.241	6.639		
Na^+–OH_2	1.878	−66.922	0.566	10.563	0.226	6.015	0.146	3.446
Na^+-NH_3	1.879	−66.682	0.570	10.625	0.224	5.945	0.144	2.740
K^+	1.880	−64.995	0.588	10.798	0.215	4.157		
LiF	1.932	−63.846	0.665	12.186	0.243	7.233	0.427	14.056
LiCl	1.926	−65.237	0.639	11.856	0.264	8.048	0.268	5.291
LiBr	1.924	−65.666	0.632	11.754	0.270	8.267	0.224	3.781
NaF	1.923	−60.645	0.705	12.511	0.177	4.401	0.299	8.361
NaCl	1.923	−61.540	0.688	12.315	0.188	4.784	0.205	3.925
NaBr	1.922	−61.772	0.683	12.263	0.190	4.836	0.177	2.955

[a] M = alkali metal. [b] M = alkali metal; X = O, N, F, Cl, Br.

+0.93e/−0.92e for HHeF–Li^+. In all complexes, this arises from a charge flux of nearly 0.15–0.20e from the fluorine to the hydrogen atom, whereas the positive charge on the helium atom remains unchanged or only slightly decreases. The increased dipole character of HHeF depends on the ligand and follows the same periodic trends already noted for the other ligand-induced structural changes of HHeF, namely, $Li^+ > Na^+ > K^+ > Rb^+ > Cs^+$, LiX > NaX (X = F, Cl, Br), and, for both LiX and NaX, Br > Cl > F. On the other hand, the charge distribution of the ligands is invariably only little affected by complexation. This suggests that the HHeF–L complexes are of ion–dipole or dipole–dipole character, and that the different shifts in charge induced in complexed HHeF essentially reflect the different polarizing ability of the alkali-metal ions and molecules (e.g., $Li^+ < Na^+ < K^+ < Rb^+ < Cs^+$). This is consistent with previous studies[40,42] that indicate that the nature of the bonding in gas-phase complexes of alkali-metal ions is essentially electrostatic (charge–dipole interaction), especially when the binding site is a first-row atom.[42] The ionic character of the interaction between HHeF and the presently investigated ligands is confirmed by the results of the AIM analysis. At the bond critical point (bcp) of any F–M bond (see Table 4), the charge density is low and the corresponding Laplacian is positive. The predicted values of ρ and $\nabla^2\rho$ range between around 0.2 and 0.4 e Å^{-3} and between around 4 and 12 e Å^{-5}, respectively, and are in general comparable with the ρ and $\nabla^2\rho$ values of the essentially purely ionic MX moieties of the HHeF–MX complexes (M = Li, Na; X = F, Cl, Br). As for HHeF, its complexation with any ligand L does not alter the covalent ($\nabla^2\rho < 0$) and ionic ($\nabla^2\rho > 0$) nature of the H–He and He–F bonds, respectively. We also note that, on passing from free to complexed HHeF, at the bcp of the H–He bond the value of ρ increases, whereas at the bcp of the He–F bond the value of ρ invariably decreases. These variations are consistent with the other structural changes induced in HHeF by complexation, namely, a shortening of the H–He distance and a lengthening of He–F distance accompanied by consistent blue- and redshifts of the H–He and He–F stretching modes, respectively.

Comparison with other related complexes: A comparison of the HHeF–L complexes investigated herein with the already investigated hydrogen-coordinated complexes of HHeF[24–27,32] suggests that the fluorine and hydrogen complexation of HHeF induce qualitatively similar structural effects. All the linear Ng–HHeF,[24,27,32] NN–HHeF,[25,32] and CO–HHeF[26,32] species feature in fact a shortening of the H–He distance, a lengthening of the He–F distance, and a consistent blue- and redshift, respectively, of the corresponding harmonic frequencies. They are also characterized by an enhanced dipole character $(HHe)^+F^-$ and electrostatic interaction energies. However, from a quantitative point of view, the effects of fluorine complexation are in general more pronounced than hydrogen complexation. At levels of theory directly comparable to those employed in this study,[24–27] the linear Ng–HHeF, NN–HHeF, and CO–HHeF feature complexation energies of only 1–3 kcal mol^{-1}, shortening of the H–He distances of between 0.005 and 0.03 Å,

lengthening of the He–F distances of between 0.04 and 0.1 Å, and corresponding frequency shifts of between +220 and +460 cm^{-1}, and −70 and −340 cm^{-1}, respectively. These comparisons are of course strongly limited by the very different character of the ligands involved in the presently comparable hydrogen- and fluorine-coordinated complexes of HHeF. In any case, it is of interest to note that the fluorine-coordinated complex HArF–HF was predicted[29,30] to be more stable than the hydrogen-coordinated HF–HArF by around 13 kcal mol^{-1}, and that the complexation energy of HArF–HF was as large as around 18 kcal mol^{-1}. In addition, for the fluorine-coordinated structure, the H–Ar distance is reduced with respect to HArF by 0.04 Å, the Ar–F distance is increased by 0.12 Å, and the corresponding harmonic frequencies are blue- and redshifted, respectively, by around 400 and 60 cm^{-1}. For the hydrogen-coordinated structure, these structural changes were invariably significantly less pronounced. Quite recently, the larger stability of the halogen-coordinated complexes of HNgY (Y = halogen atom) was confirmed by experiment. HKrCl–HCl,[43] HXeCl–HCl,[44] and HXeBr–HBr[44] were in fact observed in cold matrices together with their corresponding hydrogen-coordinated structures HX–HNgY. Based also on theoretical calculations, the halogen-coordinated structures were characterized by particularly large blueshifts of the H–Ng bonds. The blueshift of around 300 cm^{-1} of the H–Kr stretching mode of HKrCl–HCl[44] is, in particular, probably the largest blueshift experimentally observed for a 1:1 molecular complex of the noble gas hydrides. Interestingly, the halogen-coordinated complexes are invariably more stable than the hydrogen-coordinated isomers. In addition, the structural changes induced in HNgY by halogen complexation (shortening of the H–Ng distance, lengthening of the Ng-F–distance, and blue- and redshifts, respectively, of the corresponding harmonic frequencies), are qualitatively similar but quantitatively more pronounced than hydrogen complexation.

As a final note, the blueshift of the hydrogen-coordinated complexes of the noble gas hydrides HNgY was initially regarded as somewhat unusual.[45] A hydrogen bond A···H–B is in fact normally accompanied by elongation of the H–B bond and a redshift of its stretching frequency. Numerous subsequent experiments and calculations confirmed, however, that, apart from a few exceptions,[46] the contraction of the H–Ng bond and the blueshift of the corresponding frequency must be viewed as a normal effect for both hydrogen- and Y-cooordinated complexes of HNgY.[47] We confirm here this effect for the fluorine-coordinated complexes of HHeF.

Conclusion

Searching for helium compounds still remains a fascinating challenge. Although theory has so far predicted the conceivable existence of numerous cationic and dicationic covalent species,[48] the HHeF molecule is to date the only theoretical candidate for a neutral covalent helium compound. This species is intrinsically unstable, but could become indefinitely stable in solid helium at the highest pressures. To avoid such extreme conditions, it has been suggested that HHeF could be stabilized in cold matrices by complexation effects. In general, any (HHeF)L complex must be first thermochemically stable with respect to H + He + F + L. This requires large complexation energies of around 25 kcal mol^{-1}. In this study, we found that alkali-metal ions and molecules can indeed stabilize HHeF with respect to the three-body dissociation. This favorable thermochemical effect is, however, invariably accompanied by a strong decrease in the H–He–F bending barrier, which amounts to only 0.5–2 kcal mol^{-1}. Overall, our calculations cast doubt on the possible stabilization of HHeF by complexation. In any case, they disclose the first examples of fluorine-coordinated complexes of HHeF and encourage us to investigate the still little explored interaction of the noble gas hydrides HNgY with strongly electrophilic (especially cationic) species.

Computational Details

The calculations were performed with the Gaussian 03 program[49] by using the standard internal 6-311++G(2d,2p) and 6-311++G(3df,3pd) basis sets for hydrogen, helium, lithium, sodium, potassium, nitrogen, oxygen, fluorine, chlorine, and bromine. The small-core relativistic Stuttgart/Dresden (SDD) effective core potentials (ECPs) and the valence basis sets designed for these ECPs were used for rubidium and cesium.[50,51] The combinations of these basis sets are denoted here as 6-311++G(2d,2p)/SDD and 6-311++G(3df,3pd)/SDD, respectively. The geometries and harmonic frequencies of the HHeF–L complexes, of their fragments, and of the transition-state structures (TS) for their decomposition into He + HF + L were optimized at the second-order Møller–Plesset level of theory[52] (full electrons) by using the 6-311++G(2d,2p)/SDD basis set. We also optimized the geometries of the HHeF–M^+ energy minima ($M^+ = Li^+$–Cs^+) at the MP2(full) level of theory with the def2-TZVPP basis set.[53,54] Any TS located with the MP2(full)/6-311++G(3df,3pd)/SDD level of theory was unambiguously related to its interconnected energy minima by intrinsic reaction coordinate (IRC) calculations.[55] The total energies were subsequently refined by single-point calculations at the coupled cluster level of theory, CCSD(T),[56] (full electrons) performed with the 6-311++G(3df,3pd)/SDD basis set. The atomic charges were computed by natural bond orbital (NBO) analysis[57] of the MP2(full)/6-311++G(2d,2p)/SDD wave function. The effect of the basis set superposition error (BSSE) on the dissociation energies was estimated by MP2(full)/6-311++G(3df,3pd)/SDD//MP2(full)/6-311++G(2d,2p)/SDD single-point calculations using the counterpoise method of Boys and Bernardi.[58] Zero-point energies were included in all calculations using the MP2(full)/6-311++G(2d,2p)/SDD harmonic frequencies. Chemical bonding analysis was based on the theory of atoms-in-molecules (AIM) approach,[59] as implemented in AIM2000.[60] We calculated in particular the MP2(full)/6-311++G(2d,2p)/SDD charge density ρ and the Laplacian of the charge density $\nabla^2\rho$ at the bond critical points (bcp), intended as points on the attractor interaction lines where $\nabla\rho = 0$ (for a discussion about bond paths and chemical bonds see refs. [61–66]).

Acknowledgements

The authors thank the Università degli Studi di Torino, the Università della Tuscia, and the Italian Ministero dell'Università e della Ricerca

(MiUR) for financial support through the "Cofinanziamento di Programmi di Ricerca di Rilevante Interesse Nazionale".

[1] K. O. Christe, *Angew. Chem.* **2001**, *113*, 1465–1467; *Angew. Chem. Int. Ed.* **2001**, *40*, 1419–1421.
[2] M. Pettersson, J. Lundell, M. Räsänen, *Eur. J. Inorg. Chem.* **1999**, 729–737.
[3] S. Seidel, K. Seppelt, *Science* **2000**, *290*, 117–118.
[4] P. Pyykkö, *Science* **2000**, *290*, 64–65.
[5] J. Li, B. E. Bursten, B. Liang, L. Andrews, *Science* **2002**, *295*, 2242–2245.
[6] W. Grochala, *Chem. Soc. Rev.* **2007**, *36*, 1632–1655.
[7] L. A. Muck, A. Y. Timoshkin, M. v. Hopffgarten, G. Frenking, *J. Am. Chem. Soc.* **2009**, *131*, 3942–3949.
[8] J. Roithová, D. Schröder, *Angew. Chem.* **2009**, *121*, 8946–8948; *Angew. Chem. Int. Ed.* **2009**, *48*, 8788–8790.
[9] R. B. Gerber, *Annu. Rev. Phys. Chem.* **2004**, *55*, 55–78.
[10] L. Khriachtchev, M. Räsänen, R. B. Gerber, *Acc. Chem. Res.* **2009**, *42*, 183–191, and references therein.
[11] L. Khriachtchev, M. Pettersson, N. Runeberg, J. Lundell, M. Räsänen, *Nature* **2000**, *406*, 874–876.
[12] G. Frenking, *Nature* **2000**, *406*, 836–837.
[13] L. Khriachtchev, H. Tanskanen, J. Lundell, M. Pettersson, H. Kiljunen, M. Räsänen, *J. Am. Chem. Soc.* **2003**, *125*, 4696–4697.
[14] L. Khriachtchev, K. Isokoski, A. Cohen, M. Räsänen, R. B. Gerber, *J. Am. Chem. Soc.* **2008**, *130*, 6114–6118.
[15] E. Tsivion, R. B. Gerber, *Chem. Phys. Lett.* **2009**, *482*, 30–33.
[16] M. W. Wong, *J. Am. Chem. Soc.* **2000**, *122*, 6289–6290.
[17] J. Lundell, G. M. Chaban, R. B. Gerber, *Chem. Phys. Lett.* **2000**, *331*, 308–316.
[18] G. M. Chaban, J. Lundell, R. B. Gerber, *J. Chem. Phys.* **2001**, *115*, 7341–7343.
[19] T. Takayanagi, A. Wada, *Chem. Phys. Lett.* **2002**, *352*, 91–98.
[20] Z. Bihary, G. M. Chaban, R. B. Gerber, *J. Chem. Phys.* **2002**, *117*, 5105–5108.
[21] J. Panek, Z. Latajka, J. Lundell, *Phys. Chem. Chem. Phys.* **2002**, *4*, 2504–2510.
[22] T. Takayanagi, *Chem. Phys. Lett.* **2003**, *371*, 675–680.
[23] S. A. C. McDowell, *Chem. Phys. Lett.* **2004**, *396*, 346–349.
[24] A. Lignell, L. Khriachtchev, M. Räsänen, M. Pettersson, *Chem. Phys. Lett.* **2004**, *390*, 256–260.
[25] S. A. C. McDowell, *Mol. Phys.* **2004**, *102*, 71–77.
[26] S. A. C. McDowell, *J. Mol. Struct.* **2004**, *674*, 227–232.
[27] S. A. C. McDowell, *J. Mol. Struct.* **2005**, *715*, 73–77.
[28] A. Lignell, L. Khriachtchev, J. Lundell, H. Tanskanen, M. Räsänen, *J. Chem. Phys.* **2006**, *125*, 184514–184516.
[29] S. A. C. McDowell, *Chem. Phys. Lett.* **2003**, *377*, 143–148.
[30] A. V. Nemukhin, B. L. Grigorenko, L. Khriachtchev, H. Tanskanen, M. Pettersson, M. Räsänen, *J. Am. Chem. Soc.* **2002**, *124*, 10706–10711.
[31] S.-Y. Yen, C.-H. Mou, W.-P. Hu, *Chem. Phys. Lett.* **2004**, *383*, 606–611.
[32] J.-T. Wang, Y. Feng, L. Liu, X.-S. Li, Q.-X. Guo, *Chem. Lett.* **2003**, *32*, 746–747.
[33] At the MP2(full)/6-311++G(2d,2p) level of theory, the linear M–X–H–He–F (M = Li, Na; X = F, Cl, Br) were characterized as higher-order saddle points. No hydrogen-bonded energy minima were located.
[34] T. J. Lee, P. R. Taylor, *Int. J. Quantum Chem.* **1989**, *36*, 199–207.
[35] M. T. Rodgers, P. B. Armentrout, *Int. J. Mass Spectrom.* **2007**, *267*, 167–182.
[36] P. B. Armentrout, M. T. Rodgers, *J. Phys. Chem. A* **2000**, *104*, 2238–2247.
[37] J. Srinivasa Rao, T. C. Dinadayalane, J. Leszczynski, G. Naraharai Sastry, *J. Phys. Chem. A* **2008**, *112*, 12944–12953.
[38] J.-F. Gal, P.-C. Maria, L. Massi, C. Mayeux, P. Burk, J. Tammiku-Taul, *Int. J. Mass Spectrom.* **2007**, *267*, 7–23.
[39] K. E. Laidig, P. Speers, A. Streitwieser, *Coord. Chem. Rev.* **2000**, *197*, 125–139.
[40] C. Cézard, B. Bouvier, V. Brenner, M. Defranceschi, P. Milli, J. M. Soudan, J. P. Dognon, *J. Phys. Chem. B* **2004**, *108*, 1497–1506.
[41] A. M. El-Nahas, K. Hirao, *J. Phys. Chem. A* **2000**, *104*, 138–144.
[42] T. B. McMahon, G. Ohanessian, *Chem. Eur. J.* **2000**, *6*, 2931–2941.
[43] A. Corani, A. Domanskaya, L. Khriachtchev, M. Räsänen, A. Lignell, *J. Phys. Chem. A* **2009**, *113*, 10687–10692.
[44] A. Lignell, J. Lundell, L. Khriachtchev, M. Räsänen, *J. Phys. Chem. A* **2008**, *112*, 5486–5494.
[45] A. Lignell, L. Khriachtchev, M. Pettersson, M. Räsänen, *J. Chem. Phys.* **2003**, *118*, 11120–11128.
[46] S. A. C. McDowell, *Phys. Chem. Chem. Phys.* **2003**, *5*, 808–811.
[47] A. Lignell, L. Khriachtchev, *J. Mol. Struct.* **2008**, *889*, 1–11.
[48] W. Koch, G. Frenking, J. Gauss, D. Cremer, J. R. Collins, *J. Am. Chem. Soc.* **1987**, *109*, 5917–5934.
[49] Gaussian 03, Revision C.02, M. J. Frish, G. W. Trucks, H. B. Schlegel, G. E. Scuseria, M. A. Robb, J. R. Cheeseman, V. G. Zakrzevski, J. A. Montgomery, Jr., T. Vreven, K. N. Kudin, J. C. Burant, J. M. Millam, S. S. Iyengar, J. Tomasi, V. Barone, B. Mennucci, M. Cossi, G. Scalmani, N. Rega, G. A. Petersson, H. Nakatsuji, M. Hada, M. Ehara, K. Toyota, R. Fukuda, J. Hasegawa, M. Hishida, T. Nakajima, Y. Honda, O. Kitao, H. Nakai, M. Klene, X. Li, J. E. Knox, H. P. Hratchian, J. B. Cross, C. Adamo, J. Jaramillo, R. Gomperts, R. E. Stratman, O. Yazyev, A. J. Austin, R. Cammi, C. Pomelli, J. W. Ochterski, P. Y. Ayala, K. Morokuma, G. A. Voth, P. Salvador, J. J. Dannenberg, V. G. Zakrzewski, S. Dapprich, A. D. Daniels, M. C. Strain, O. Farkas, D. K. Malick, A. D. Rabuck, K. Raghavachari, J. B. Foresman, J. V. Ortiz, Q. Cui, A. G. Baboul, S. Clifford, J. Cioslowski, B. B. Stefanov, G. Liu, A. Liashenko, P. Piskorz, I. Komaromi, R. L. Martin, D. J. Fox, T. Keith, M. A. Al-Laham, C. Y. Peng, A. Nanayakkara, M. Challacombe, P. M. W. Gill, B. G. Johnson, W. Chen, M. W. Wong, C. Gonzalez, J. A. Pople, Gaussian, Inc., Wallingford, CT, **2004**.
[50] I. S. Lim, P. Schwerdtfeger, B. Metz, H. Stoll, *J. Chem. Phys.* **2005**, *122*, 104103–104115.
[51] The pseudopotentials (ECP28MDF for rubidium and ECP46MDF for cesium) and the corresponding basis sets were downloaded from http://www.theochem.uni-stuttgart.de/pseudopotentials.
[52] C. Møller, M. S. Plesset, *Phys. Rev.* **1934**, *46*, 618–622.
[53] F. Weigend, R. Ahlrichs, *Phys. Chem. Chem. Phys.* **2005**, *7*, 3297–3305.
[54] T. Leininger, A. Nicklass, W. Kuechle, H. Stoll, M. Dolg, A. Bergner, *Chem. Phys. Lett.* **1996**, *255*, 274–280.
[55] C. Gonzalez, H. B. Schlegel, *J. Phys. Chem.* **1990**, *94*, 5523–5527.
[56] K. Raghavachari, G. W. Trucks, J. A. Pople, M. Head-Gordon, *Chem. Phys. Lett.* **1989**, *157*, 479–483.
[57] NBO Version 3.1, E. D. Glendening, A. E. Reed, J. E. Carpenter, F. Weinhold, Theoretical Chemistry Institute, University of Wisconsin, Madison.
[58] S. Boys, F. Bernardi, *Mol. Phys.* **1970**, *19*, 553–566.
[59] R. F. W. Bader, *Atoms in Molecules: a Quantum Theory*, Oxford University Press, Oxford, **1990**.
[60] AIM2000, F. Biegler-König, University of Applied Sciences, Bielefeld, http://www.AIM2000.de.
[61] J. Cioslowski, S. T. Mixon, *J. Am. Chem. Soc.* **1992**, *114*, 4382–4387.
[62] A. Haaland, D. J. Shorokhov, N. V. Tverdova, *Chem. Eur. J.* **2004**, *10*, 4416–4421.
[63] A. Krapp, G. Frenking, *Chem. Eur. J.* **2007**, *13*, 8256–8270.
[64] a) J. Poater, M. Solà, F. M. Bickelhaupt, *Chem. Eur. J.* **2006**, *12*, 2902–2905; b) J. Poater, R. Visser, M. Solà, F. M. Bickelhaupt, *J. Org. Chem.* **2007**, *72*, 1134–1142.
[65] a) E. Cerpa, A. Krapp, A. Vela, G. Merino, *Chem. Eur. J.* **2008**, *14*, 10232–10234; b) E. Cerpa, A. Krapp, R. Flores-Moreno, K. J. Donald, G. Merino, *Chem. Eur. J.* **2009**, *15*, 1985–1990.
[66] R. F. W. Bader, *J. Phys. Chem. A* **2009**, *113*, 10391–10396.

Received: November 30, 2009
Published online: April 15, 2010

